Management of Solid Waste Marble Powder: Improving Quality of Sodium Chloride Obtained From Sulphate Rich Lake/Subsoil Brines With Simultaneous Recovery of High Purity Gypsum and Light Basic Magnesium Carbonate

Rahul J. Sanghavi
CSIR-Central Salt and Marine Chemicals Research Institute
Sumesh C. Upadhyay
CSIR-Central Salt and Marine Chemicals Research Institute
Arvind Kumar (arvind@csmcri.res.in)
Central Salt and Marine Chemicals Research Institute CSIR https://orcid.org/0000-0001-9236-532X

Research Article

Keywords: Solid waste, marble dust powder, lake brine, salt, gypsum, light basic magnesium carbonate

Posted Date: November 30th, 2021

DOI: https://doi.org/10.21203/rs.3.rs-1026571/v1

Abstract

Marble industry worldwide produces large amount of non-degradable marble dust powder (MDP) waste during mining and processing stages. MDP mainly comprises of $CaCO_3$ with small amounts of Mg, Fe or Si in various forms. In India, mainly in Rajasthan state, marble is quarried in huge amounts and MDP thus produced is collected improperly and dumped at any abandoned land or identified disposal sites leading to several environment hazards. On the other hand, the composition of sub soil/lake brines of Rajasthan is typical in nature as it does not have much Ca^{2+} and Mg^{2+} impurities but contains higher levels of SO_4^{2-}. Therefore, the common salt (NaCl) produced from such brines is contaminated with Na_2SO_4 (8-30 wt%) depending upon SO_4^{2-} concentration in the brine. Such a salt produced is neither suitable for edible purpose nor for industrial usage. Herein, we have reacted MDP with HCl, and the resulting solution ($CaCl_2$ and $MgCl_2$ slurry) is used in stoichiometric ratio of Ca^{2+} to SO_4^{2-} in brines to produce high purity NaCl and gypsum ($CaSO_4{\cdot}2H_2O$) via fractional crystallization. Remaining magnesium containing solution was reacted with Na_2CO_3 to prepare high purity light basic magnesium carbonate hydrate. Purity of crystallized NaCl, $CaSO_4{\cdot}2H_2O$ and $MgCO_3{\cdot}6H_2O$ has been ascertained through analytical and spectral methods (TGA, FTIR, P-XRD). Field emission scanning electron microscopy (FE-SEM) was used to elucidate morphology of crystals. The method reported for improving purity of NaCl along with $CaSO_4{\cdot}2H_2O$ and $MgCO_3{\cdot}6H_2O$ production from sulphate rich brines is simple and economic, and allow management of MDP generated in huge amounts, which poses problems of disposal and creates environment hazards.

Introduction

Marble is a metamorphic rock composed of recrystallized carbonate minerals, most commonly calcite or dolomite (Philip, 2001). Metamorphism causes variable recrystallization of the original carbonate mineral grains. The purest calcite ($CaCO_3$) marble is white in color. Reddish, yellowish or greenish colour in marbles is mainly due to hematite (Fe_2O_3), limonite ($FeO(OH){\cdot}nH_2O$) or serpentine $(Mg, Fe)_3\ Si_2O_5(OH)_4$ respectively. Marble has been prized for its use in sculptures or as a construction material (Ferrari; Han et al., 2018; M, 2004). India is fourth largest marble producer in the world after Italy, China and Spain respectively. Out of the total production in India, approximately 85% is quarried from Rajasthan state generating roughly around 5-6 Million Metric Tons of MSD slurry every year. Various options, such as utilization in cement manufacturing (Aruntaş et al., 2010; Ashish et al., 2016; Khichi, 2017; Toubal Seghir et al., 2019), production of synthetic gypsum through chemical reaction (DOLEŽELOVÁ et al., 2017; Krejsová et al., 2019), utilization in road construction (Chandra et al., 2002; Rai et al., 2020) as a low cost binder, (Khan et al., 2020) or in brick manufacturing (Emir et al., 2011; Gencel et al., 2012; ur Rehman, 2014) have been explored to manage this huge inorganic waste in a productive manner.

However, utilization of MDP for improving the quality of solar salt with simultaneous production of gypsum from high sulphate rich brines, such as Rajasthan lake brines has not been explored so far. Makrana, Kishangarh, Rajsamand, Alwar are some of the important marble processing centres in the

state which are in the vicinity of saline water lakes (Sambhar and Didwana) where common salt is produced with higher impurities of sodium sulphate. The calcite marble rocks of Makrana have calcium oxide and magnesium oxide in the range of 39-47% and 4-8% respectively whereas dolomite rocks of Rajsamand and Kishangarh regions have CaO and MgO in the range of 26-44% and 16-22% respectively. MDP generated while processing such rocks when reacted with a mineral acid can produce water-soluble inorganic calcium or magnesium based salts solutions. Such salt solutions when mixed with sulphate rich brine are suitable for precipitation of gypsum prior to obtaining high purity solar salt and preparation of magnesium chemicals after the recovery of common salt.

Rajasthan is third largest salt producing state in India, after Gujarat and Tamil Nadu, by contributing 10-12 % of total Indian salt production. Rajasthan has no seacoast, and therefore, solar salt production is exclusively dependent on sub-soil/lake brine in the area. Composition of brine of this region is typical and different with sea brine as it does not have much calcium and magnesium impurities but contains high level of sulphate impurities. The major impurities being sodium sulphate (in the form of Glauber salt, i.e. $Na_2SO_4.10\ H_2O$) which seems easy to remove by simple washing with fresh water to achieve good quality of salt. However, Rajasthan having hot climate, this Glauber salt turns to anhydrous Na_2SO_4, which has a less solubility and is very difficult remove from salt just by washing. Thus higher percentage of sodium sulphate leads to low purity salt and therefore difficult to cop up with edible or industrial grade salt specifications. Moreover, during solar salt production, the manufacturers recycle the bittern (left over mother liquor after the separation of salt) back to the weak brine and go on feeding the same bittern every time, which on the contrary increases the concentration of Na_2SO_4 in the brine. After certain concentration, Na_2SO_4 not only starts floating on the surface of the brine and reduces the rate of evaporation of the brine, but also results in deteriorated quality of salt.

Many processes have been reported for the production of sodium chloride with lesser impurities. These methods include both chemical and biological interventions in brine systems (Mishra et al., 2004). In order to improve the quality of salt, common ion effects have been utilized to crystallize gypsum from brines forcibly by addition of calcium chloride or sodium sulphate (Hamidani and Sanghavi, 1992; Vohra et al., 2004). Such practices were not found practical in salt fields as large quantities of calcium chloride or sodium sulphate are to be added and thus making process tedious and economically unviable. In order to make salt manufacturing process economically viable, cost effective sources of calcium chloride such as soda ash distiller waste which has significant amounts of $CaCl_2$ and NaCl have been used for desulphatation of subsoil brine (Vohra et al., 2004). Such a practice not only improved the quality and yield of salt but also helped in mitigation of the problems of environmental discharge of effluent in water bodies. However, such a process is more practical when soda ash plants are available near solar salt works. Therefore, we have utilized MDP, which is in abundance in the vicinity of Rajasthan lake brines for improving the quality of salt along with the recovery of high purity gypsum. The remaining solution after recovery of salt and gypsum contain high magnesium content, therefore, magnesium recovery makes the process more significant. Magnesium in the form of its carbonate salt is widely needed in industrial process of paints, ceramics, cosmetics, pharmaceuticals, preparation of paper and other magnesium

based chemicals. Magnesium carbonate can be precipitated in several forms which include hydromagnesite, nesquehonite or magnesite etc. (Lou et al., 2004). Magnesium carbonate recovery has been reported using Uyuni Salar brine (Tran et al., 2016), using polyacrylamide (Guo et al., 2010), from reaction between magnesium hydroxide and carbon dioxide (Han et al., 2014), from magnesium chloride solution (Hao and Al-Tabbaa, 2014), or by reacting sea bitterns with sodium chloride (Apriania et al., 2018). Herein, we have recovered magnesium carbonate by reacting magnesium rich liquor with sodium carbonate, thus making the process very economic. Common salt, gypsum and magnesium carbonate have been characterized using different techniques in terms of purity and yield.

Materials And Methods

Marble dust powder (MDP) was collected from a marble processing industry located in Rajsamand, Rajasthan. Commercial Grade Hydrochloric acid (11 N) was procured from DCM Shriram Ltd. (Shriram Alkali & Chemicals; CAS number: 7647-01-0), Kota, Rajasthan which is near Didwana Lake. Sulphate rich brine of Didwana lake was used as source of NaCl and Na_2SO_4. Lake brine, MDP, slurry generated after reaction of MDP with HCl, and crystallized salts were analysed using standard volumetric, gravimetric or flame photometry techniques (Trivedi et al., 2014), Mg^{2+} and Cl^- concentrations were determined volumetrically using standard EDTA and $AgNO_3$ solutions and SO_4^{2-} was determined gravimetrically using $BaCl_2$, with an error of <0.2%. Na^+ and K^+ ions were analysed with the help of digital flame analyser (Cole-Parmer, Model 2655-00). Various salts crystallized were characterized using PerkinElmer GX FTIR spectrometer (10 scans with a resolution of 4 cm^{-1} were made). TGA measurements were performed using a TGA/SDTA851 Mettler Toledo under a nitrogen atmosphere from 0 to 800°C with a heating rate of 10°C min^{-1}. XRD pattern was recorded using Philips X'pert MPD XRD diffractometer and morphology of precipitated crystals was investigated using FE-SEM (JFM 7100 F; Oxford Inc.) the adopting procedure reported in earlier paper (Shukla et al., 2018).

Results And Discussions

The sub-soil brine was analysed in order to establish its density and ionic composition. The chemical analysis is provided in Table 1 and Table 2.

Table 1 Ionic composition of Didwana Lake brine

Specific gravity (SG)	^{0}Bé	Ca^{2+} % (w/v)	Mg^{2+} (%w/v)	SO_4^{2-} (%w/v)	Cl^- (%w/v)	K^+ (%w/v)	CO_3^{2-} (%w/v)	HCO_3^- (%w/v)
1.1436	18.2	Nil	0.0004	3.49	8.75	0.03	0.18	0.61

Table 2
Probable composition of salts dissolved Didwana Lake brine

Na_2SO_4 (%w/v)	$MgCl_2$ (%w/v)	KCl (%w/v)	NaCl (%w/v)	Na_2CO_3 (%w/v)	$NaHCO_3$ (%w/v)
5.17	0.0014	0.07	14.38	0.32	0.84

It has been observed that lake brine has higher sulphate content as compared to the sea brine at similar density. Table 1 shows, that 1 L of lake brine contains 34 g of SO_4^{2-} at 18.2°Bé [°Bé =145×[1-(1/SG)] whereas sea brine analysis shows 13.5 g sulphate at a similar density, with a probable concentration of nearly 5 (w/v) % of Na_2SO_4 along with 14 (w/v) % of NaCl (Table 2). Lake brine has also very low content of Mg^{2+} and Ca^{2+} as compared to the seawater. The common salt has been crystalized from this brine via solar evaporation method. The composition of salt crystallized is given in Table 3. As can be seen from Table 3, the salt is highly contaminated with Na_2SO_4 (23.46 % w/w) which is very difficult to wash, and not suitable either for edible or industrial application.

Table 3
Chemical analysis of salt obtained Didwana Lake brine

$CaSO_4$ (%w/w)	Na_2SO_4 (%w/w)	$MgCl_2$ (%w/w)	NaCl (%w/w)	KCl (%w/w)	Na_2CO_3 (%w/w)	$NaHCO_3$ (%w/w)
0.03	23.46	0.09	74.05	0.05	2.08	0.24

The dolomite rocks of have CaO and MgO in the range of 26-44% and 16-22% respectively. Therefore, MDP generated while processing such rocks was reacted with HCl to generate water-soluble inorganic calcium or magnesium based salts solutions and insolubles. In a typical experiment, 321 g of marble powder was dissolved 535 ml HCl (11 N) and kept overnight for preparation of slurry/solution. Insolubles residue (59 g) was filtered and salt slurry (542 ml) thus obtained was analysed for chemical composition (Table 4, Table 5).

Table 4 Chemical analysis of salt slurry obtained by mixing of MDP and HCl

Ca^{2+}(%w/v)	Mg^{2+} (%w/v)	SO_4^{2-} (%w/v)
10.39	6.16	0.099

Table 5 Probable composition of salts in the slurry obtained by mixing of MDP and HCl

$CaCl_2$ (%w/v)	$MgCl_2$ (%w/v)	$CaSO_4$ (%w/v)	acid insoluble (%w/v)
28.72	24.09	0.14	18.38

Therefore, the filtered slurry (225 ml) was used as economic additives in lake brine (1500 ml brine) to make a stoichiometric proportion of Ca^{2+} to SO_4^{2-}. Composition of the resulting brine is given in Table 6.

Table 6 Ionic composition of lake brine after addition of slurry obtained by mixing of MDP and HCl

°Bé	Ca^{2+} (%w/v)	Mg^{2+} (%w/v)	SO_4^{2-} (%w/v)	Cl^- (%w/v)	K^+ (%w/v)
18.8	0.19	0.78	0.69	9.61	0.03

Resulting solution was subjected to solar evaporation to crystallize $CaSO_4 \cdot 2H_2O$ and improve quality and yield of NaCl. $CaSO_4 \cdot 2H_2O$ fraction was crystallized between 18.8 to 24.0°Bé, and analysed for chemical composition and purity.

Table 7 Ionic and probable composition of $CaSO_4 \cdot 2H_2O$ fraction collected between 18.8 - 24.0°Bé

Ionic Composition					
°Bé	Ca^{2+} (%w/w)	Mg^{2+} (%w/w)	SO_4^{2-} (%w/w)	Cl^- (%w/w)	K^+ (% w/w)
18.8 - 24.0	19.80	0.61	48.86	2.42	Nil
Probable Composition					
°Bé	$CaSO_4.2H_2O$ (%w/w)	$MgSO_4$ (%w/w)	$MgCl_2$ (%w/w)	KCl (%w/w)	NaCl (%w/w)
18.8 - 24.0	85.14	1.68	1.06	Nil	2.69

As can be seen from Table 7, $CaSO_4 \cdot 2H_2O$ with a purity of higher than 85 (%w/w) could be directly precipitated and purity was improved up to 96 (%w/w) by washing the soluble impurities with a weak brine. Purity of gypsum crystals were examined using P-XRD and FTIR (Figure 1left, right). The XRD pattern of precipitated $CaSO_4 \cdot 2H_2O$ (Figure 1left) showed prominent peaks with d-spacing at 7.55, 4.26, 3.79, and 3.06 Å which are comparable with corresponding d-values of 7.52, 4.25, 3.76, and 3.05Å reported in literature (Follner et al., 2002). The vibrational spectral characteristics of the precipitated gypsum crystals are shown in Figure (1right). The absorption bands at 602, 669 and 1117 cm^{-1} correspond to the different modes of SO_4^{2-}. Presence of H_2O in gypsum is confirmed from the band around 1630 cm^{-1} and the broad band around 3400 cm^{-1} (Prasad et al., 2005).

Morphology of crystals was examined by FE-SEM (Figure 2). SEM images have shown that crystals have grown from soft spongy dumble or spherical shaped to tabular pseudo-hexagonal and rigid. EDX spectra shows some minor impurities of sodium chloride which can be easily washed away by simple washing

After $CaSO_4 \cdot 2H_2O$ recovery, brine was further concentrated up to 29°Bé and pure NaCl was collected between 24 to 29 °Bé. Analysis of NaCl (ionic and probable composition) crystallized between 24 to 29°Bé is provided in Table 8 and 9.

Table 8 Ionic composition of NaCl fractions collected between 24.0-29.0^{o}Bé

^{o}Be'	Ca^{2+} % (w/w)	Mg^{2+} % (w/w)	SO_4^{2-} % (w/w)	Cl^{-} % (w/w)	K^{+} % (w/w)
24.0 - 25.0	0.25	0.17	0.66	58.88	0.03
25.0 - 26.0	0.46	0.29	1.18	57.17	0.01
26.0 - 27.0	0.33	0.51	1.08	57.86	0.01
27.0 - 28.0	0.06	0.57	0.49	59.67	0.04
28.0 - 29.0	0.12	0.67	2.84	58.31	0.04

Table 9 Probable composition of NaCl fractions collected between 24.0-29.0^{o}Bé

^{o}Bé	$CaSO_4$ (%w/w)	$MgSO_4$ (% w/w)	$MgCl_2$ (%w/w)	KCl (%w/w)	NaCl (%w/w)
24.0 - 25.0	0.87	0.08	0.60	0.05	98.39
25.0 - 26.0	1.62	0.12	1.09	0.02	97.15
26.0 - 27.0	1.19	0.36	1.81	0.03	96.61
27. 0 - 28.0	0.20	0.44	1.92	0.07	97.37
28.0 - 29.0	0.41	3.20	0.13	0.07	96.19

The purity of as such collected NaCl was always > 96 %w/w meeting specifications of edible grade salt, which could be further improved to > 98.5 %w/w by simple washing with water and meeting industrial grade salt specifications. Purity of washed salt has been ascertained from P-XRD pattern and FTIR spectra of unwashed and washed samples (Fig. 3 left, right).

Morphology of crystallized NaCl indicated growth of crystals from hollow to dense cubic structures (Figure 4). EDX spectra shows a very high purity of the crystallized salt. After separation of NaCl at 29^{o}Bé filtrate was recovered and analysed for Mg^{2+} content (Table 10).

Table 10 Ionic and probable composition of filtrate at 29.0^{o}Bé

Ionic Composition					
^{o}Bé	Ca^{2+} (%w/v)	Mg^{2+} (%w/v)	SO_4^{2-} (%w/v)	Cl^- (%w/v)	K^+ (% w/v)
29.0	0.03	5.57	2.30	20.99	0.23
Probable Composition					
^{o}Bé	$CaSO_4$ (%w/v)	$MgSO_4$ (%w/v)	$MgCl_2$ (%w/v)	KCl (%w/v)	NaCl (%w/v)
29.0	0.11	2.78	19.59	0.43	10.22

Filtrate contained approximately 5.6 (%w/v) of Mg^{2+}, which is quite suitable to recover magnesium salts economically. From magnesium rich solutions, different types of magnesium carbonate hydrates can be synthesized by carefully adjusting the reaction temperature and pH value of the initial reaction solution in the precipitation process. Magnesium carbonate normally crystallizes in the di-, tri-, or pentahydrates ($MgCO_3{\cdot}2H_2O$, $MgCO_3{\cdot}3H_2O$ or $MgCO_3{\cdot}5H_2O$) which are colourless crystals having triclinic and monoclinic structures. Therefore, we used magnesium rich filtrate to crystallize magnesium carbonate hydrate. $MgCO_3{\cdot}6H_2O$ was prepared using a known quantity of Na_2CO_3 and was separated from sodium chloride solution. In a typical experiment, clear Na_2CO_3 solution was added to the dilute bittern in stoichiometric ratios of magnesium to carbonate. The precipitated slurry of hydrated $MgCO_3$ was stirred and then allowed to stand. Slurry was put under filtration and washed with fresh water to make it free from chloride and sulphate. Wet cake was then dispersed in fresh water such that the slurry concentration is reduced. This dispersion was heated to 50–60^{o}C and maintained at this temperature for 30 minutes to transform into dried basic magnesium carbonate. The complete integrated scheme of crystallization of gypsum, sodium chloride and magnesium carbonate is shown in Figure 5.

During investigations it has been found that a rare form of magnesium carbonate hexahydrate ($MgCO_3{\cdot}6H_2O$) has been crystallized (Rincke et al., 2020). $MgCO_3{\cdot}6H_2O$ formed was analysed for chemical composition (Table 11), and characterized for its bulk density, moisture content, purity and morphology.

Table 11 Ionic composition of precipitated light basic $MgCO_3{\cdot}6H_2O$

Sample details	Mg (% w/w)	Ca (% w/w)	Cl (% w/w)	MgO (% w/w)	CaO (% w/w)	KCl (% w/w)
$MgCO_3$ unwashed	17.84	0.98	15.48	29.61	1.37	0.04
$MgCO_3$ Washed	26.18	0.06	0.26	43.46	0.08	0.03

Based on the above analysis purity of washed $MgCO_3.6H_2O$ was found to be > 98.5 % w/w. Bulk density of the washed sample was found to be 130.50 and 217.50 g/l for loose and pack respectively, meeting the criteria of light basic $MgCO_3$ suitable for industrial applications.

The product was initially characterized using TGA in order to assess water of hydration (Figure 6). TGA profiles indicated small weight loss up to 110^oC indicating loss of moisture and the process of decomposition starts at around 100^oC and completes around 500^oC. The thermograms indicated that the weight loss occurred in different stages, about 60 wt%. In first stage, up to 160^oC around 14.9 wt% loss occurs, between 160 to 280^oC approx. 12.4 wt% and between 280 to 500^oC approx. 33.6 wt% loss occurs. After a calculation from the weight loss in different temperature stages of the TGA curve, the material obtained have a simple formula of $MgCO_3{\cdot}6H_2O$. The purity of product was further characterized using PXRD.Figure 5 (left) shows the PXRD pattern of product phase which matches with the magnesium carbonate hexahydrate ($MgCO_3{\cdot}6H_2O$) reported (Rincke et al., 2020) and complements the results obtained from TGA profiles. PXRD pattern of product phase $MgCO_3{\cdot}6H_2O$ in comparison with the reference data for $MgCO_3{\cdot}3H_2O$ (Nesquehonite, 98-016-9540) is provided in Figure 7 (right).

Figure 8 shows the IR spectra of crystallized $MgCO_3{\cdot}6H_2O$. IR spectra is very similar to those of $MgCO_3{\cdot}3H_2O$ which is confirmed by the presence of ~850 cm^{-1} (υ2 mode), 1117 cm^{-1} (υ1 mode), 1485 and 1426 cm^{-1} (υ3 mode) CO_3^{2-} adsorption bands (Farmer, 1974; White, 1971; Zhang et al., 2006). The CO_3^{2-} asymmetric stretching vibrations are observed as a strong band split in two at 1485 and 1426 cm^{-1} cm^{-1} (υ3 mode) (Sawada et al., 1978). In addition, a faint band around 1645 cm^{-1} corresponding to the O-H bending mode of water. Broad bands in the range of 3650-3000 cm^{-1} corresponds to O-H of water molecules in the compound. These bands have much difference between them, which is likely originating from a different number of water of crystallization. A sharp band around 3650 cm^{-1} is assigned to the free O-H vibration (Zhang et al., 2006).

Morphology of crystals depends upon several conditions viz. composition of reaction mixture, reaction temperature, carbonation time, pH of the solution etc. Figure 9 provides a set of typical SEM images of a dried sample under the investigated conditions. Here, fine nano-sized thick plates like particles are produced which arrange into small rod like structures. Elemental analysis and EDX spectra shows a very high purity of the crystallized magnesium carbonate (Figure 9).

Techno economic analysis

Based on the common salt, magnesium carbonate and gypsum production production rates and chemical input requirements, techno economic feasibility of production of 1 ton/day capacity plant is evaluated (Table 12). The economic viability of salts produced has been assessed based on the following economic indicators: Plant establishment costs: capital expenditure (CAPEX); Operating expenditure (OPEX); Cost recovery from struvite production (revenue). Equipment sizes based on the mass production and cost estimation of the process equipment has been estimated as provided in Table 13. The viability calculations have been done based on pilot scale experiments.

Table 12 Basic engineering design of common salt, magnesium carbonate and gypsum production

Capacity of the Plant (TPA) – Common Salt	**3540**
Capacity of the Plant (TPA) - Magnesium Carbonate	300
Capacity of the Plant (TPA) - Gypsum	1166
Basis	2 shifts/day, 300 Working days per annum
Design Basis	10% Design Margin
Capital Cost (Rs. in lakhs)	110.95
Annual Sales Revenue (Rs. in lakhs)	194.36
Annual Profit Before Tax	28.83
Pay Back Period (Years)	3.83
Return on Capital Investment	22.19%
Break Even Point	39.36%
Assumptions:	
Economic life of plant	10 Years
Construction Period	6 months
Capacity Utilisation	75% - 1st Year; 85% - 2nd Year; 100% - 3rd Year onwards

Table 13 Total capital investment (TCI)

Sr.No.	Description	Amount (Rs. in lakhs)
1	Civil Works	12.88
2	Plant & Equipment	86.74
3	Furniture & Fixtures	2.00
4	Laboratory & QC Equipment	5.00
	Grand Total	110.95

Raw materials cost as estimated according to actual consumption from pilot experimental results and prevailing costs, other components of operating costs are presented in Table 14. The rates of raw material and utilities mentioned below are prevailing rates in market. Standard norms have been taken for depreciation, maintenance and repair cost which are applicable for chemical plant.

Table 14 Raw material and utilities consumption and production cost

Description	Rate, Rs. per unit	Consumption per MT of $MgCO_3$	Total cost per annum (Rs. In lakhs)
Raw Material			
Hydrochloric Acid (M^3)	1500	10	44.46
Marble dust (MT)	1000	6	17.79
Sub Soil Brine (M^3)	10	65	1.96
Na_2CO_3 (MT)	25000	1	79.01
Total			143.23
Utilities (in Plant only)			
Electricity (KWH)	7.5	132.97	2.99
Water	10	22	0.65
Total			3.64
Salaries & Wages			9.18
Depreciation	5% of Plant & Equipment, 10% of civil work		5.62
Maintenance & Repair	2.5% of Plant & Equipment, 1.5% of civil work		2.36
Packing Cost			1.50
Grand Total			165.53
Sales revenue	Rate (Rs. per unit)	Unit	
Salt (Sodium Chloride)	500	3540 (TPA)	17.70
Magnesium Carbonate	55000	300 (TPA)	165.00
Gypsum	1000	1166 (TPA)	11.66
Total (Rs. in lakhs)			194.36
Profit before tax (Rs. In lakhs per annum)			28.83

Manpower requirements with their monthly and annual remunerations for running of plant are given below in Table 15.

Table 15 Manpower requirement

Description	No.	Monthly Salary (Rs.)	Months	Annual Salary (Rs.)
Supervisor	1	15000	12	180000
Plant Operator	1	12500	12	150000
Unskilled worker	3	10000	12	360000
		Total		690000
Fringe Benefit @33%				227700
Total				917700

Return on capital investment costing has been done with the assumptions that the economic life of equipment is ten years, two-shift per day basis and no bank borrowings for capital expenditures. The calculations are provided in Table 16.

Table 16 Return on capital investment

Profit before tax over 10 years' period (Rs. in lakhs)	246.22
Average Annual Operating Surplus (Rs. in lakhs)	24.62
Capital Investment (Rs. in lakhs)	110.95
Return on Capital Investment	22.19%

Break even analysis has been done with 100% capacity utilization which is normally achieved during third year of operation. It has been assumed that capacity utilization during first and second year will be 75% and 80% respectively. The calculations are given in Table 17.

Table 17 Break even analysis (Based on 3rd year of operation L.E. 100% capacity utilization)

Items	Cost break up	
	Fixed	Variable
Raw Materials & Utilities	0.00	146.87
Packing materials	0.00	1.50
Salaries & Wages	10.12	0.00
Maintenance & Repairs	2.36	0.00
Depreciation	5.62	0.00
Total	18.10	148.37
Annual Sales Revenue (Rs. in lakhs)	= 194.36	
Break Even Point	= 18.10 x 100	
	194.36 - 148.37	
	= 39.36%	

Payback period was calculated based on six years of operation using net surplus and cumulative net surplus amounts and is provided in Table 18.

Table 18 Payback period

Year of operation	Net Surplus (Rs. in lakhs) (i.e. Profit + Depreciation)	Cumulative Net Surplus (Rs. in lakhs)
1	22.95	22.95
2	27.09	50.05
3	33.51	83.56
4	33.01	116.57
5	32.47	149.04
6	31.92	180.96
Capital Investment (Rs. Lakhs) =	110.95	
		110.95 - 116.57
Payback period =	4 +	
		149.04 - 116.57
=	3.83 Years	

Techno-economic analysis indicates that production of common salt, magnesium carbonate and gypsum will generate enough revenue to recover the cost of production and make profit with a payback period of approximately 4 years. Recovery of salts in current process is thus concluded to be technically feasible and the economically affordable.

Conclusions

We have shown that large amount of non-degradable marble dust powder (MDP) generated from marble industry during mining and processing stages can be used for improving quality and yield of salts produced from sulphate rich lake/sub-soil brines. MDP has been reacted with HCl to generate slurry comprising of Ca^{2+} and Mg^{2+} ions, which was added directly to lake/sub-soil brines in stoichiometric ratios of Ca^{2+} to SO_4^{2-} in brine. Subsequent brine was subjected to solar evaporation for crystallization of high purity gypsum and common salt. The remaining Mg^{2+} rich liquor was processed for preparation of light basic magnesium carbonate in the form of a rare phase $MgCO_3 \cdot 6H_2O$. Chemical, spectral and morphological analysis indicates that various salts are precipitated with a very high purity suitable for industrial applications. Studies indicate that the method of MDP utilization in lake/sub-soil brines in stoichiometric ratios can not only mitigate the environment hazards of solid waste discharge but can help in improving the quality of crystallized salts (gypsum and sodium chloride) in solar salt works along with recovery of value added magnesium salts in an economical manner.

Declarations

Acknowledgement

Communication number, CSIR-CSMCRI-197/2021. Authors are thankful to Mr. Rakesh Dobariya for his assistance during experimental work. The analytical facilities of institute are acknowledged for sample characterizations.

Conflict of interest

The authors declare that they have no conflict of interest.

Ethics approval and consent to participate

Not applicable

Consent to Publish

Not applicable

Authors Contributions

Rahul J. Sanghavi: experimental work, methodology, and analysis. Sumesh C. Upadhyay: Techno economic analysis of the process. Arvind Kumar: conceptualization, supervision and writing-reviewing

and editing.

Funding

CSIR India through CSIR-CSMCRI in-house projects MLP 0029 and MLP 0050.

Availability of data and materials

All data generated or analysed and materials used and produced during this study are included in the article.

References

1. Apriania M, Hadia W, Masduqia A (2018) Synthesis of Magnesium Carbonate Polymorphs from Indonesia Traditional Salt Production Wastewater. Environment Asia 11:140–148
2. Aruntaş HY, Gürü M, Dayı M, Tekin I (2010) Utilization of waste marble dust as an additive in cement production. Mater Design 31:4039–4042
3. Ashish DK, Verma SK, Kumar R, Sharma N (2016) Properties of concrete incorporating sand and cement with waste marble powder. Advances in concrete construction 4:145
4. Chandra S, Kumar P, Feyissa BA (2002) Use of marble dust in road construction. Road Materials and Pavement Design 3:317–330
5. DOLEŽELOVÁ M, VIMMROVÁ KREJSOVÁJ, A (2017) Lightweight gypsum based materials: Methods of preparation and utilization. International Journal of Sustainable Development and Planning 12:326–335
6. Emir E, Konuk A, Daloğlu G (2011) Strength enhancement of Eskisehir tuff ashlars in Turkey. Constr Build Mater 25:3014–3019
7. Farmer VC (1974) Infrared spectra of minerals. Mineralogical society
8. Ferrari A PROCEEDINGS 4th International Congress on “Science and Technology for the Safeguard of Cultural Heritage in the Mediterranean Basin” VOL. I. Angelo Ferrari
9. Follner S, Wolter A, Helming K, Silber C, Bartels H, Follner H (2002) On the real structure of gypsum crystals. Crystal Research and Technology: Journal of Experimental and Industrial Crystallography 37:207–218
10. Gencel O, Ozel C, Koksal F, Erdogmus E, Martínez-Barrera G, Brostow W (2012) Properties of concrete paving blocks made with waste marble. J Clean Prod 21:62–70
11. Guo M, Li Q, Ye X, Wu Z (2010) Magnesium carbonate precipitation under the influence of polyacrylamide. Powder Technol 200:46–51
12. Hamidani A, Sanghavi J, IMPROVEMENT IN THE QUALITY OF SALT FROM INLAND BRINE OF KHARAGHODA AREA (1992) Research and Industry 37:46–48

13. Han B, Qu H, Niemi H, Sha Z, Louhi-Kultanen M (2014) Mass transfer and kinetics study of heterogeneous semi-batch precipitation of magnesium carbonate. Chem Eng Technol 37:1363–1368
14. Han S, Cui Y, Huang H, An M, Yu Z (2018) Effect of curing conditions on the shrinkage of ultra high-performance fiber-reinforced concrete. Advances in Civil Engineering 2018
15. Hao R, Al-Tabbaa A (2014) A CCS mineralization process: Investigation of the production of magnesium carbonates from magnesium chloride solution. Energy Procedia 63:8017–8025
16. Khan MA, Khan B, Shahzada K, Khan SW, Wahab N, Ahmed M (2020) Conversion of waste marble powder into a building material. Civil Engineering Journal 6:431–445
17. Khichi ESK (2017) Effect of Calcitic Marble Dust Powder on Cement Concrete
18. Krejsová J, Schneiderová Heralová R, Doleželová M, Vimmrová A (2019) Environmentally friendly lightweight gypsum-based materials with waste stone dust. Proceedings of the Institution of Mechanical Engineers, Part L: Journal of Materials: Design and Applications 233, 258-267
19. Lou Z, Chen Q, Zhu Y, Zhang Y, Gao J (2004) Growth of Magnesium Carbonate Single Crystal in Supercritical Carbon Dioxide– Molten Sodium System. Cryst Growth Des 4:415–417
20. M J (2004) Marble Institute of America Glossary, 223
21. Mishra S, Ghosh PK, Gandhi MR, Bhatt AM, Chauhan SA (2004) Process for the removal of calcium ions from the brine by marine cyanobacteria. Google Patents
22. Philip K (2001) Dictionary of geology. Penguin Group, London and New York
23. Prasad P, Chaitanya VK, Prasad KS, Rao DN (2005) Direct formation of the γ-CaSO4 phase in dehydration process of gypsum: In situ FTIR study. Am Mineral 90:672–678
24. Rai P, Pei H, Meng F, Ahmad M (2020) Utilization of marble powder and magnesium phosphate cement for improving the engineering characteristics of soil. International Journal of Geosynthetics and Ground Engineering 6:1–13
25. Rincke C, Schmidt H, Voigt W (2020) A new hydrate of magnesium carbonate, MgCO3· 6H2O. Acta Crystallographica Section C: Structural Chemistry 76:244–249
26. Sawada Y, Uematsu K, Mizutani N, Kato M (1978) Thermal decomposition of hydromagnesite 4MgCO3-Mg (OH) 2-4H2O under different partial pressures of carbon dioxide. Thermochimica acta 27:45–59
27. Shukla J, Mehta MJ, Kumar A (2018) Effect of ionic liquid additives on the solubility behavior and morphology of calcium sulfate dihydrate (gypsum) in the aqueous sodium chloride system and physicochemical solution properties at 30 C. Journal of Chemical & Engineering Data 63:2743–2752
28. Toubal Seghir N, Mellas M, Sadowski Ł, Krolicka A, Żak A, Ostrowski K (2019) The utilization of waste marble dust as a cement replacement in air-cured mortar. Sustainability 11:2215
29. Tran KT, Han KS, Kim SJ, Kim MJ, Tran T (2016) Recovery of magnesium from Uyuni salar brine as hydrated magnesium carbonate. Hydrometallurgy 160:106–114
30. Trivedi TJ, Shukla J, Kumar A (2014) Effect of Nitrate Salts on Solubility Behavior of Calcium Sulfate Dihydrate (Gypsum) in the Aqueous Sodium Chloride System and Physicochemical Solution

Properties at 308.15 K. Journal of Chemical & Engineering Data 59:832–838

31. ur Rehman W (2014) Utilization of marble waste slurry in the preparation of bricks. Journal of the Pakistan Institute of Chemical Engineers 42:47–54
32. Vohra RN, Ghosh PK, Mohandas VP, Joshi HL, Deraiya HH, Dave RH, Halder K, Yadav RB, Daga SL, Majeethia KM (2004) Recovery of common salt and marine chemicals from brine. Google Patents
33. White WB (1971) Infrared characterization of water and hydroxyl ion in the basic magnesium carbonate minerals. American Mineralogist: Journal of Earth and Planetary Materials 56, 46-53
34. Zhang Z, Zheng Y, Ni Y, Liu Z, Chen J, Liang X (2006) Temperature-and pH-dependent morphology and FT– IR analysis of magnesium carbonate hydrates. J Phys Chem B 110:12969–12973

Figures

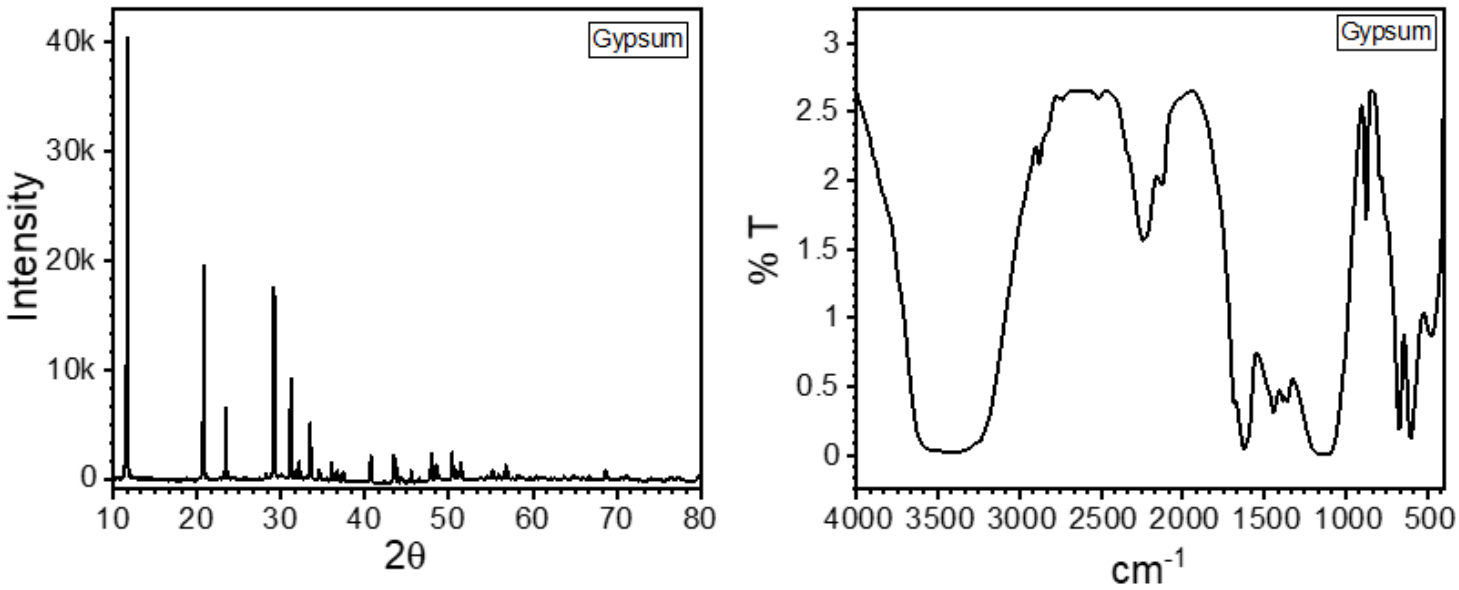

Figure 1

(left) P-XRD pattern and (right) FTIR spectra of washed CaSO4·2H2O.

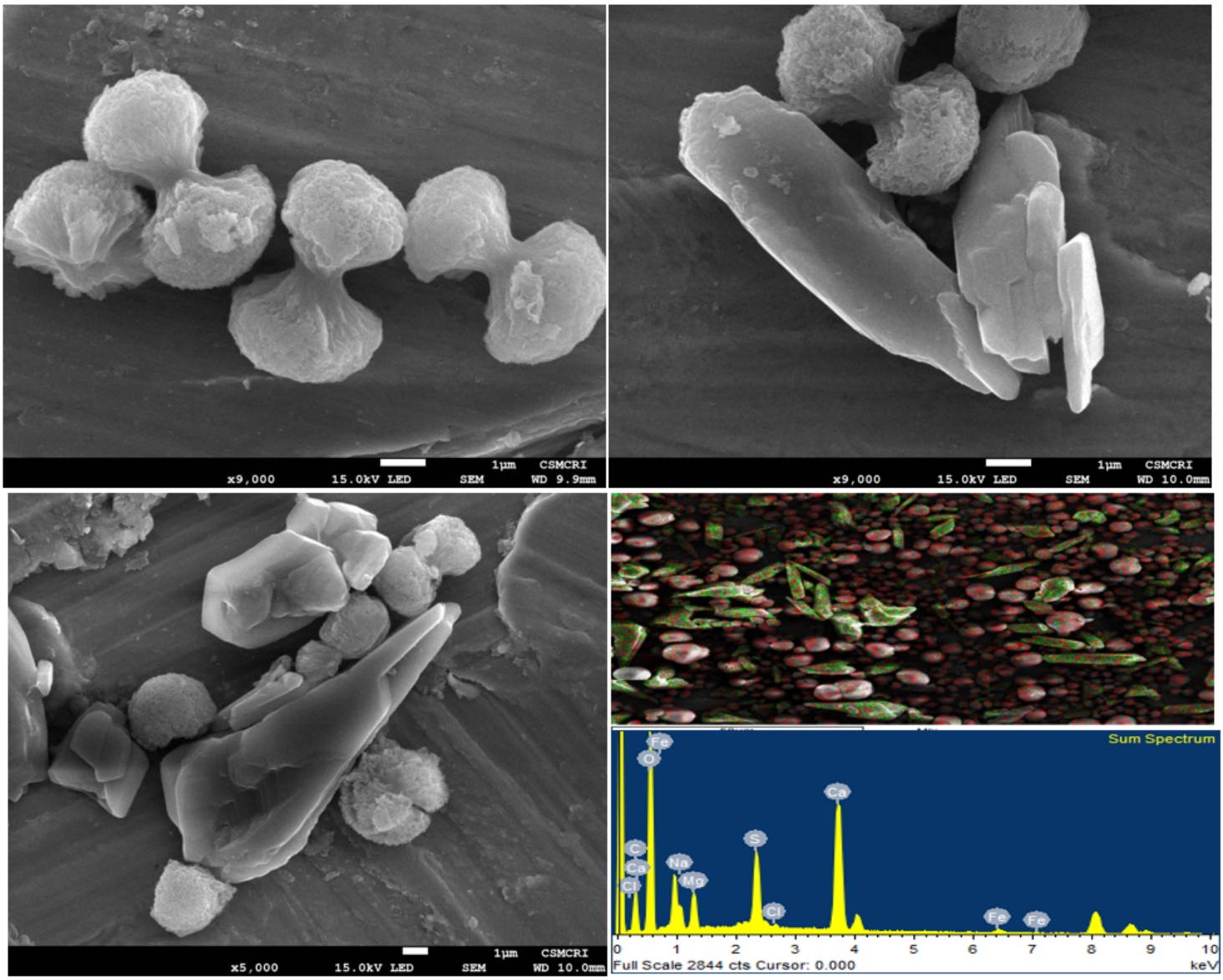

Figure 2

SEM images and EDX spectra of CaSO4·2H2O precipitated from lake brine after addition MDP slurry.

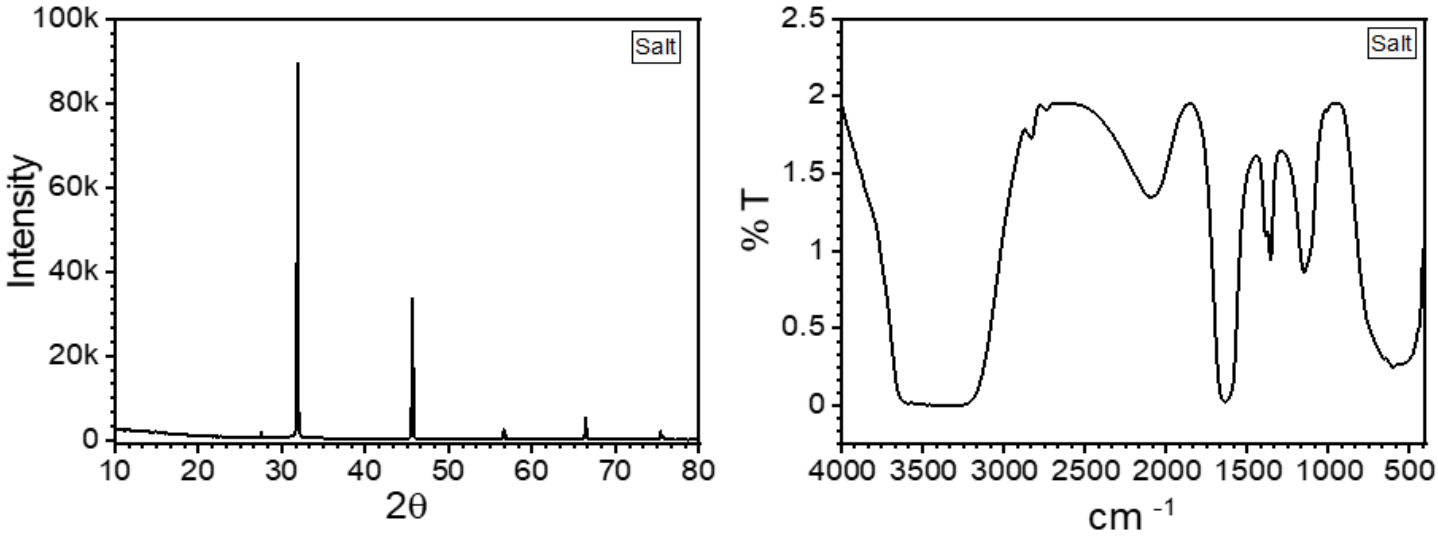

Figure 3

(left) P-XRD pattern and (right) FTIR spectra of washed NaCl

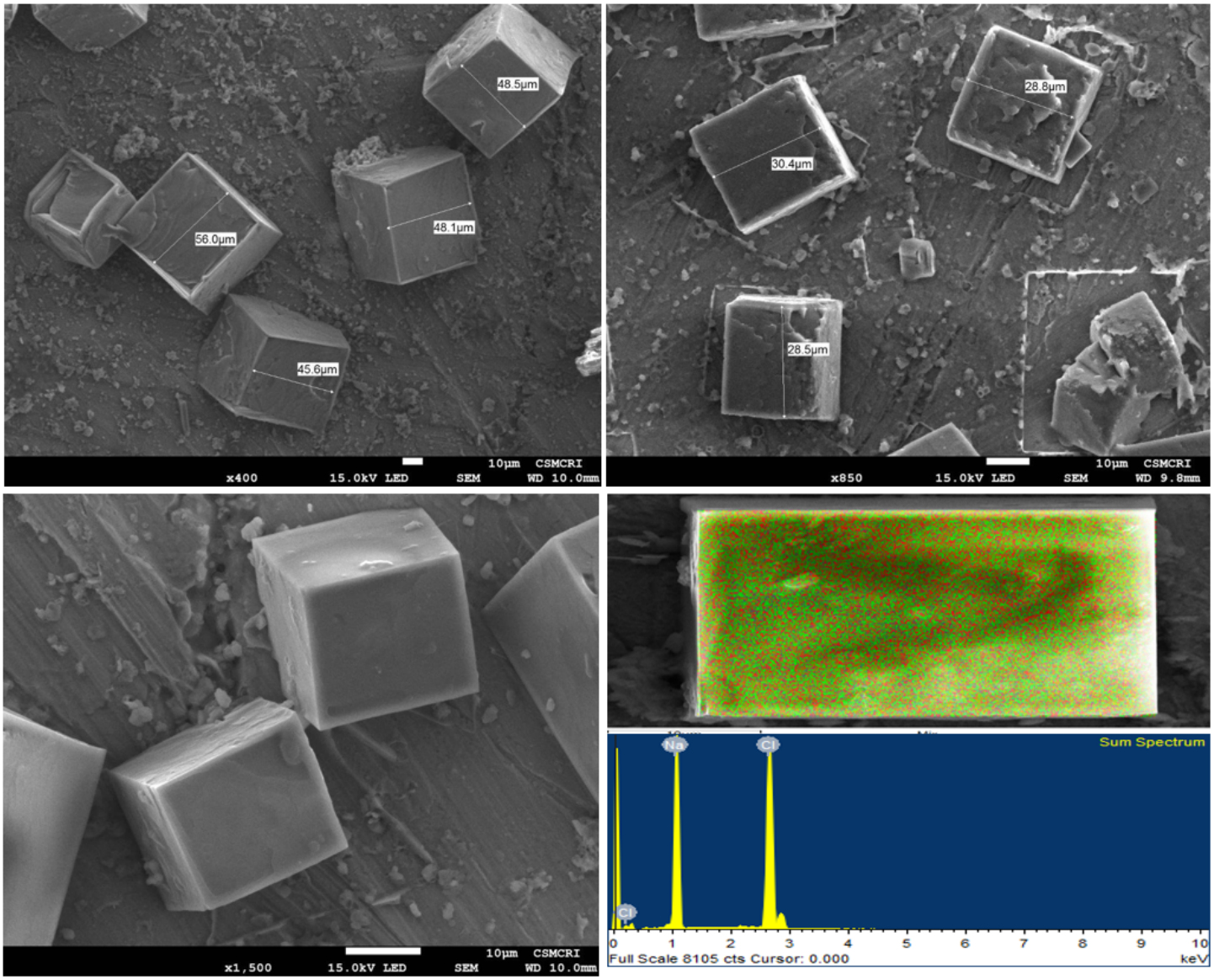

Figure 4

SEM images and EDX spectra of NaCl crystallized from lake brine after addition MDP slurry.

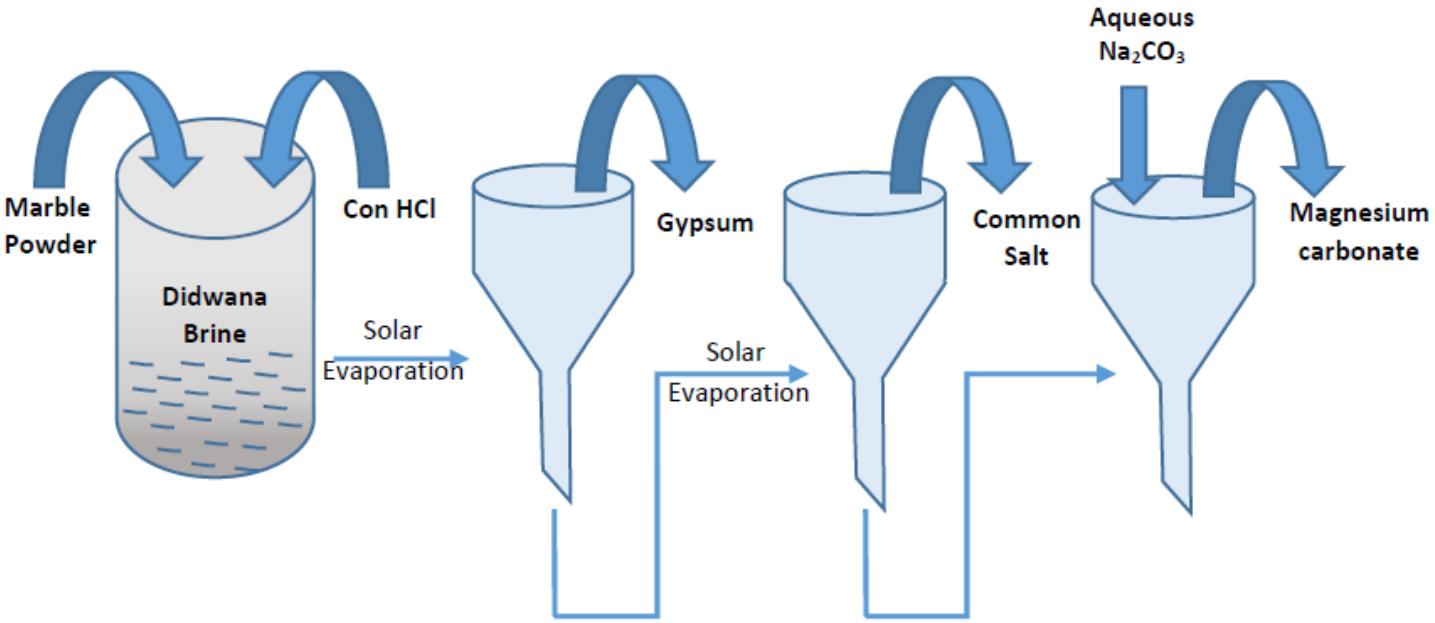

Figure 5

Schematic of recovery of high purity NaCl, CaSO4·2H2O and MgCO3·6H2O from sulphate rich lake brines using marble dust powder.

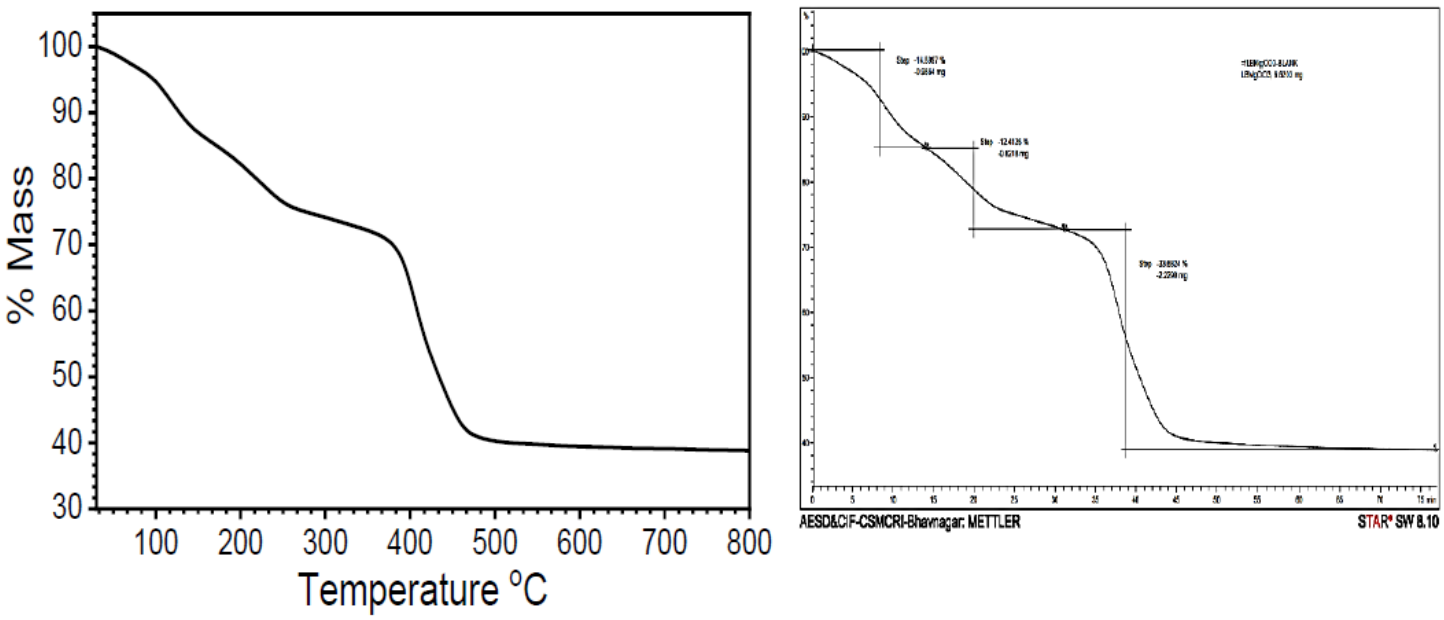

Figure 6

TGA profile of MgCO3·6H2O prepared from magnesium rich filtrate after recovery of common salt (left) weight loss vs. temperature (right) weight loss vs. time as recorded during measurements.

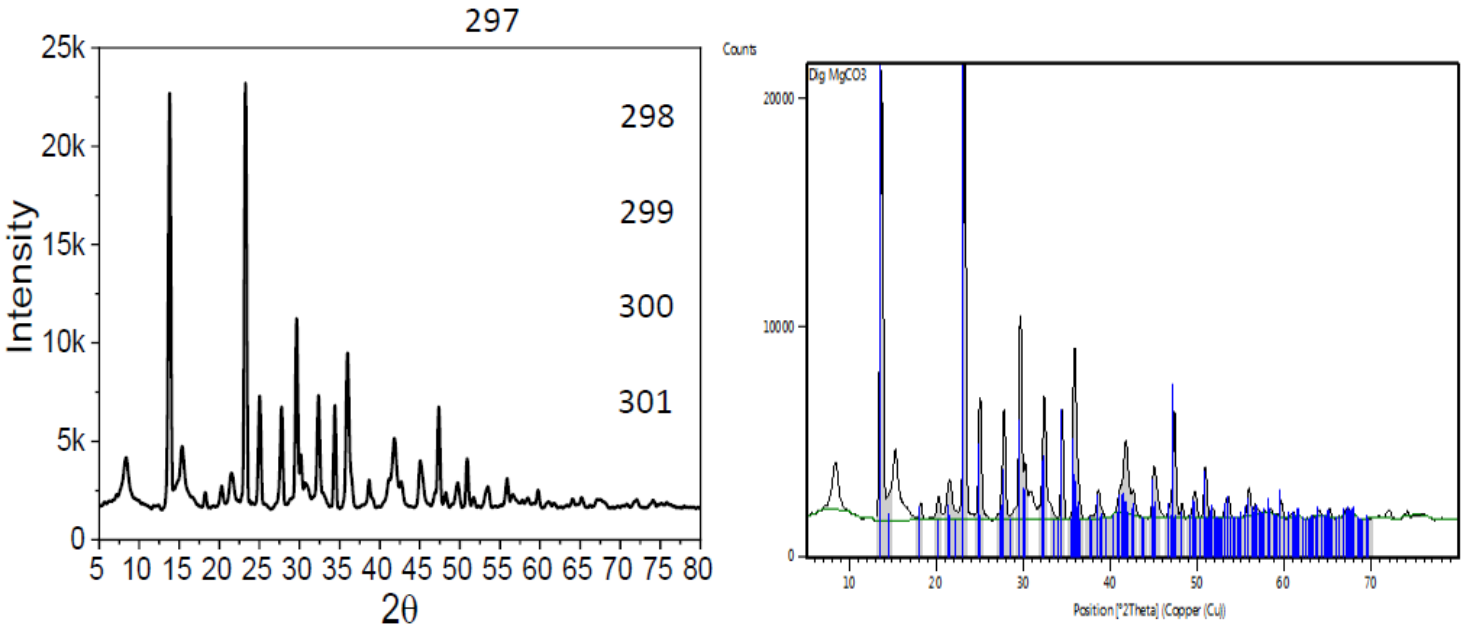

Figure 7

(left) PXRD pattern of MgCO3·6H2O prepared from magnesium rich filtrate after recovery of common salt (right) PXRD pattern of MgCO3·6H2O overlapped with reference data (Nesquehonite, 98-016-9540).

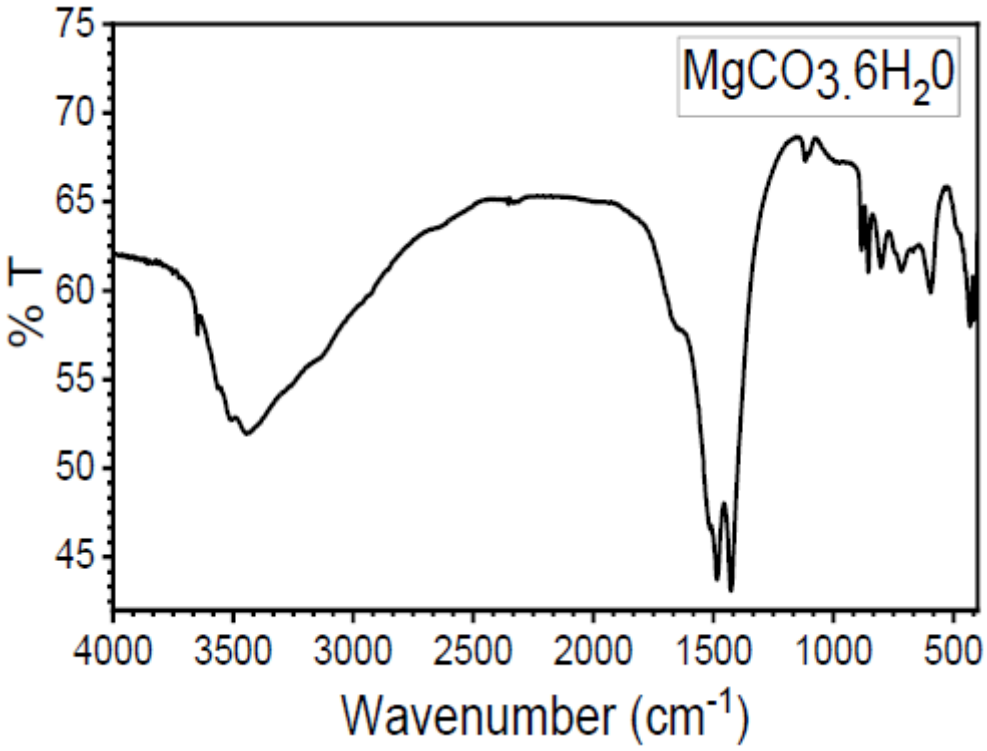

Figure 8

FTIR spectra of MgCO3·6H2O prepared from magnesium rich filtrate after recovery of common salt.

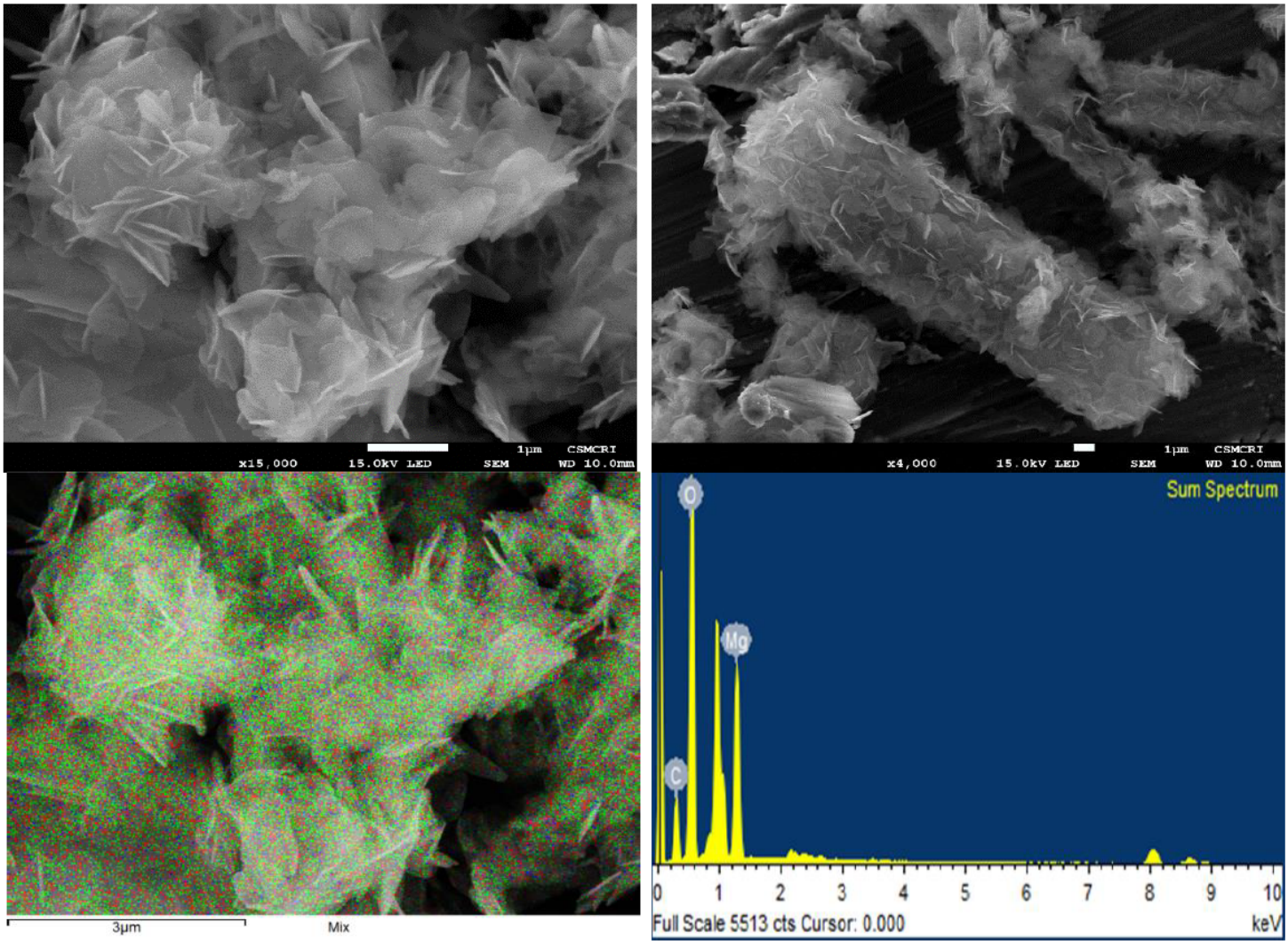

Figure 9

SEM images, elemental mapping and EDX spectra of MgCO3·6H2O prepared from magnesium rich filtrate after recovery of common salt.